Journal of **N**onlinear **A**nalysis and **O**ptimization
Vol. 16, Issue. 1: 2025
ISSN : **1906-9685**

MACHINIABILITY CHARCTERISTICS OF HOT AIR ABRASIVE JET MACHINING

Dr.S. Rajendra Prasad[1], D.Rishendra[2] , N.Vamsi Krishna[3], S.Dinesh[4] , Sk.Hamraj[5]
[1]Associate Professor, Dept. of Mechanical Engineering, Audisankara College of Engineering and Technology
[3,4,5,6] B.Tech Student, Dept. of Mechanical Engineering, Audisankara College of Engineering and Technology
[1)] siddagunta.raja@gmail.com

Abstract
Now a days many manufacturing firms are dealing with complicated in machining mediums are stainless steels, alloys, carbides, high temperature steels, etc. lots of those mediums also discover critical programs in firms to gives importance to their hardness to high power weight ratio, and warmth combat character. Although con temporized scientific advancements, unconventional machining strategies continue insufficient to device those materials in view of gainful production, besides machining of those mediums into complicated shapes is time ingesting and sometime not possible. Non-conventional machining strategies have emerged to triumph over those difficulties. The primary machining precept of Abrasive hot Air Jet Machining is that the abrasive debris are multiplied through a compressed high stress warm air and are forced via a micro nozzle which collides with tough and brittle paintings portions at a very high velocity and density. for the reason that fabric elimination manner of AHAJM is done by an integration of brittle machining based totally on micro crack propagation, there's very little chipping and crack era inside the paintings piece. therefore, this method could be very appropriate for the slicing of micro shapes of hard and brittle materials (along with glass, ceramics, silicon and many others.). To present investigation focuses on determining MRR and surface roughness when hot air temperature is varied from 300C to 500C, SOD (5, 6, 7mm) and pressure of jet (4, 5, 6kgf/cm2). From the results it can be concluded that MRR and Ra are more significant with increase in temperature.
Keywords: AHAJM, Soda lime glass, Sic (abrasive particles), MRR, surface roughness

1 INTRODUCTION
1.1 NON-TRADITIONAL MACHINING:

The primary approach of traditional machining predominantly revolves around the elimination of materials through the utilization of tools that exhibit greater hardness compared to the materials being worked on. However, the application of traditional machining techniques often proves inadequate when it comes to working with newly developed materials that possess enhanced chemical, mechanical, and thermal attributes. Moreover, traditional machining practices tend to be inefficient when applied to the machining of rigid substances such as ceramics and composites or when operating within extremely stringent tolerances, as observed in micro machined components like aerospace and electronics industries.

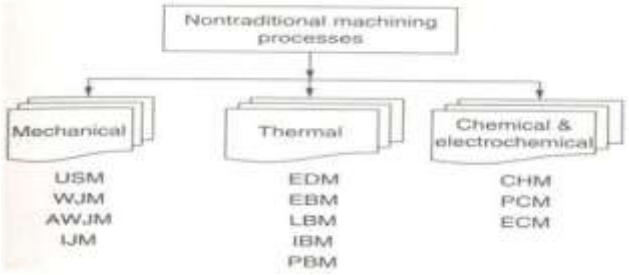

Fig 1.1: Classification of Non-Traditional Machining

The abrasive used in abrasive jet machining is much finer, and the process parameters and cutting action are both carefully controlled. This process is primarily used to cut intricate shapes in hard, brittle materials that are heat-sensitive and prone to chipping. Abrasive jet machining can also drill, deburr, and clean. It avoids chatter and vibration issues common with physical tools. The cutting remains cool since the carrier gas acts as a coolant, removing heat.

2. Literature Review

Achtsnick et al. [1]. investigation of particle exits velocities in the air flow and modelling of the micro abrasive blasting process for various nozzle types.

Balasubramaniam et al. [2] looked into a number of factors that influence how an AJM-machined surface turns out.

El-Domiaty et al. [3], demonstrated AJM drilled glass plates of various thicknesses to ascertain their machinability under various regulating conditions (air pressure, air flow rate).

Ramachandran and Ramakrishnan [4], the AJM works well with brittle, hard materials like ceramics and glass. Mirrors and window glass are two examples of fragile materials that can be decorated or texturized with the AJM.

In order to improve the jet's efficiency in micro-grooving, Zhang et al. [5] have developed statistical models for the prediction and process optimization of Micro Abrasive Intermittent Jet Machining (MAIJM), as well as an intermittent jet mechanism.

Park et al. [6], U-type geometries can be seen in the machined profiles of the grooves. It has been found that when the nozzle was inclined with regard to the target surface, the erosion rate depended on the jet scanning direction.

Ghobeity et al [7] presented models to predict the profiles of AJM for basic shapes like channels, holes, and planar areas.

Fan et al [8] utilized dimensional analysis technique to develop a mathematical model for the erosion rate in hole and channel machining on glass using micro abrasive air jet.

Shafiei et al [9] developed a computer simulation model to predict the shape and size of erosion profile in AJM process, demonstrating good agreement between predicted and measured eroded profiles at low particle flux.

Slikkerveer et al. [10] recently proposed a powder blasting process as a fast and simple mechanical etching method for fabricating micro systems in brittle materials.

Zhou and Bahadur et al [11] reported that the erosion rate in alumina ceramics is influenced by temperature, which affects material properties and micro structure. However, limited research has been conducted on hot air jet machining. Glass cutting with an impinging hot air jet is a non-conventional technique that relies on establishing a thermal stress field in the glass to enable stable propagation of a preexisting crack.

Muralidhar et al [12] have proven that the cutting of glass material can also be performed using only hot air jet is developed a compact portable hot air jet gun for thermal cutting of glass plate and the effect of various parameters on cutting rate has been discussed.

Shahani and Seyyedian[13] conducted a study on the modelling and simulation of cutting glass plates using a hot air jet. They utilized finite element analysis and found that a specific minimum air temperature is necessary for the initiation and continuation of the cutting process, within an acceptable range of nozzle height from the glass sheet.
Previous researchers on the AJM process have not extensively explored carrier media, as revealed by the literature survey.
This article aims to address this gap by utilizing hot air as the carrier media in AJM. An abrasive hot air jet was developed, and the impact of air temperature on material removal rate (MRR) and surface roughness was examined. The morphology of the machined surface and the mechanism of material removal were analysed using SEM micro graphs.

3. Methodology

AHAJM is a basic machining process in which hot air is forced at high velocities and densities through a nozzle onto the surface of the work piece to accelerate the abrasives. The work piece used in this work is soda-lime glasses of the appropriate size for the cutting process. Samples are washed and degreased, and weighed before the test. The final weight of the samples is measured by digital electronic balance using four measurements per sample. The average value of the final reading is then calculated using a digital weight machine. The loss of mass per unit time of each specimen is then calculated and the material removal rate (MRR) is calculated. The roughness of the part is measured by surface roughness testers at four different places, and the average of the roughness (Ra) is taken as roughness of the surface.

The sensors are utilized to measure the air temperature at the nozzle exit. The air temperature in close proximity to the nozzle tip is regarded as either the air temperature or the jet temperature.

In this particular research, only significant and easily manageable variables such as air temperature, stand-off distance, and work piece thickness were taken into account. The remaining experimental parameters remained constant during the entire machining process

4 EXPERIMENTAL SETUPS OF AHAJM

"The primary elements utilized in abrasive hot air jet machining included the following:"

4.1 single- stage reciprocating air compressor and Delivery system:

This system ensures a continuous supply of clean and dry gas for propelling the abrasive particles. Depending on the needs of the setup, either an air compressor or bottled gas can be utilized. If an air compressor is chosen, it is essential to install proper line filters to prevent water or oil contamination of the abrasive powders. The most commonly used gases, which are also the least expensive, are nitrogen and carbon dioxide. It is important to note that oxygen should never be used due to the potential fire hazard it poses. The air is introduced into the system through the control valve from the air compressor, where the airflow is regulated and the required amount of air is released. The air compressor is equipped with a pressure measuring instrument that provides the operating or working pressure of the air. From the compressor, the air flows through a flexible tube and passes through heating and FRL units before reaching the mixing chamber. The delivery system consists of rubber hoses that connect the air compressor, which serves as the gas propulsion system, to the working chamber via the mixing chamber. The specifications of a single stage reciprocating air compressor can be found in the provided table.

Fig 4.1: Single- stage reciprocating air compressor

Table 4.1: Compressor Specifications

Dia. of piston	70 mm
Stroke	90 mm
Operating Pressure	8 kgf / cm^2

Speed	700 rpm
Power	3 HP
Energy Meter Constant	300 rev/kwh

4.2 Filter regulator lubricatorunit:

It is installed between the compressor and the heating unit to remove water and oil from compressed air. The reason for this is that abrasives have a property to remove the water content and the oil content.

Fig 4.2: Filter regulator lubricator unit

Table 4.2: Filter regulator lubricator unit specifications:

Material	Aluminium
Operating Pressure	Upto 8 Bar
Weight	Up to 432 g
Operating Temperature	5 To 60 degree C
Surface Finishing	Polished

4.3 Heating unit with control panel:

The compressed air is heated by this component, which is positioned between the compressor and the mixing chamber.

Fig 4.3: Heating unit with control panel

An electric heater is a device that utilizes an electric current to generate heat. Within each electric heater, there is a heating element composed of an electrical resistor. This heating element operates based on the principle of Joule heating, where the passage of an electric current through a resistor result in the conversion of electrical energy into heat energy. The majority of contemporary electric heating devices employ nichrome wire as the active element, which is supported by ceramic insulators.

Table 4.3: Heating unit with control panel specifications

Power Consumption	2000 (Watts)
Product Length	15 (cm)
Product Width	10 (cm)
Product Height	6 (cm)
Product Weight	1.5 (kg)

The specifications of a heating unit with control panel is shown in the table 4.3

4.4 Infrared Thermometer:

Fig 4.4: IR Thermometer

Infrared Thermometers utilize advanced technology to measure the emitted energy of objects. Using a combination of lenses and mirrors, these thermometers are able to accurately focus the infrared energy onto a highly sensitive detector. This detector then converts the captured energy into an electrical signal, which is then translated by the thermometer into a precise digital temperature reading.

4.5 Mixing chamber:

The fabrication process involves a cylindrical container that serves as a mixing chamber for combining air and abrasive materials. This crucial component is securely positioned on the horizontal bed. Two openings are present on opposite sides of the mixing chamber. Within the mixing chamber, the dry air and abrasives are thoroughly blended before being directed into the working chamber through the outlet opening.

Fig 4.5: Mixing chamber

The details regarding the mixing chamber's specifications and the specific material utilized for its manufacturing can be found in table 4.4.

Table 4.4: Mixing chamber specifications

Type of Material	CI
Length	150 mm
Diameter	100 mm
Thickness	3.5 mm
Operating pressure	20 bar

4.6 Working Chamber:

The machining operation will take place within a cuboidal metal casing. To prevent splashing, the chamber is enclosed on three sides. A conical funnel is welded to the bottom of the cuboidal structure to collect the used abrasives and chips

Fig 4.6 (a): Working Chamber

The vice in the working chamber is equipped with a lead screw, while the base of the cuboidal structure holds the lead screw. The cutting operation is made possible by the cross-feed movement of the vice. On top of the working chamber, a flange and thread pipe fitting are installed to adjust the nozzle distance. This fitting is constructed using mild steel sheet. The amplitude of the vibration in the mixing chamber determines the feed rate of the abrasive particles. Gas or air flow and pressure are regulated by a pressure regulator. To control the shape and size of the cut, various well-designed mechanisms such as cam mechanism, pantograph, and mechanism can be used to move either the work piece or the nozzle.

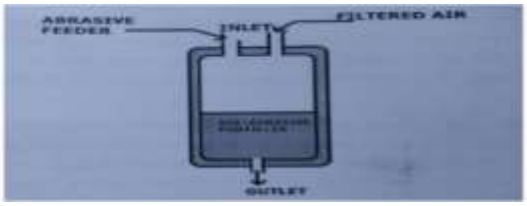

4.6(b): mixing chamber of air and abrasive particles

4.7 Pressure gauge:

These are positioned at the appropriate positions to measure the necessary pressures at the required points.

Fig 4.7: Pressure gauge

Pressure gauge is a mechanical instrument designed to measure the internal pressure and / or vacuum of the system. Amazingly, pressure gauges come in a variety of designs, sizes, and materials for the wetted parts to meet the needs of both standard and custom applications.

Table 4.5: Pressure gauges Specifications:

Accuracy	±2%
Range	0 to 14kg/Sqcm
Dial Size	2"
Case & Bazzel Coated	Drawn Steel black Powder

4.8 Nozzle and work table:

AJM nozzle is a cylindrical mouthpiece that is connected to the end of a pipe. Its main purpose is to convert the pressure head into the kinetic head, which results in a substantial increase in fluid flow at the outlet.

Table 4.6: Specifications of nozzle:

Type of Material	SS
Nozzle inlet diameter	10 mm
Nozzle outlet diameter	4 mm
Angle of taper	20 degrees
Length of Nozzle	25 mm

AJM nozzles can be made of either tungsten carbon or sapphire. Tungsten carbon nozzles come with round or rectangular holes, and have an average life of 33 hours. However, round nozzles are much more expensive, ranging from 3 to 8 times higher. For this study, we are using a 4mm stainless steel nozzle. The worktable is made of CI material.

Fig 4.8: Nozzle and worktable

Table 4.7: Specifications of worktable:

Type of Material	CI
Diameter	150.0 mm

4.9 Assembled abrasive jet machine setup without heating unit:

Fig 4.9: Assembled abrasive jet machine setup

Hose pipes and clamps are then used to connect all the parts. First, compressor is connected with FRL unit, which acts as a filter, regulator, and lubricator. Next, FRL is connected with heating unit, which has a control panel. Finally, abrasive container is connected with the pipes. From the output of the abrasive container, a pipe is connected to the nozzle, which will allow the compressed air and the abrasive mixture to be transported to the nozzle. In between the abrasive container output and the nozzle, a 2-Way valve is connected to the pipe to regulate the flow rate of the abrasive mixture, as shown in Fig 4.9.

Then two pressure gauges are attached to the pipe before and after the valve. The assembled abrasive hot air jet machining setup is shown in the fig 4.10.

4.11 Weighing machine and surface roughnesstester: Weighing machines are used to measure the work piece weight. To use a scale, the item which needs to be weighed is put on one side of the scale.

Types of Weighing Scales

1. Strain gauge load cells.
2. Force Motor Scales.

3. Acryl motor precision scales.

4.10 Assembled abrasive hot air jet machine setup:

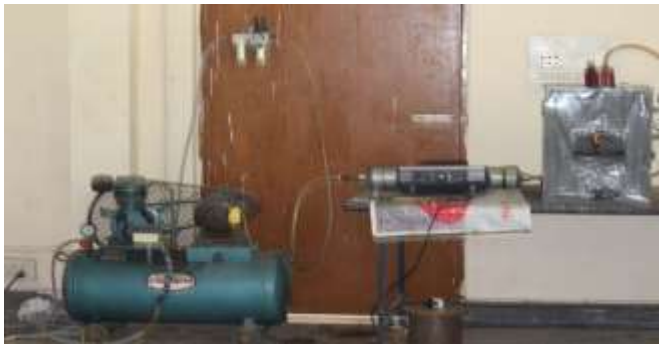

Fig 4.10: Assembled abrasive hot air jet machine setup

Fig 4.11: Weighing machines and surface roughness tester

4.11 Surface roughness testers:

A roughness tester measures the surface texture, or surface roughness, of a material. It shows the roughness depth measured (Rz) and the average roughness value measured (Ra) in millimetres (µm).

4.12 Materials:

In the current study, soda-lime glass and Sic were utilized as the work material and abrasive particles, respectively. Aluminium oxide, a commonly used abrasive, is employed for cleaning, cutting, and deburring. On the other hand, silicon carbide, a harder abrasive, is effective for the same applications as aluminium oxide but is typically used when the work piece material is very hard. Glass beads are used for polishing surfaces to a Matt finish or peening surfaces, making them suitable for heavier cleaning and peening operations. Abrasives are available in various sizes, with the smaller sizes being more useful for polishing and cleaning, while the larger sizes are better for cutting and peening. The appropriate size of specimen was used for the grooving process. Prior to machining, the specimens were washed, degreased, and weighed. After the test, the samples were cleaned with pressurized air and their final weight was measured using a digital electronic balance with a resolution of 0.1mg. Four measurements were taken for each sample, and the average value was considered as the final reading. The weight loss per unit time for each specimen was calculated and referred to as the Material Removal Rate (MRR). Additionally, the roughness of the machined part was measured using a surface roughness tester (Surf Test SJ201P, Mitutoyo, Japan). The average roughness value (Ra) of the machined part was recorded at four different locations, and the mean value was

considered as the surface roughness. The temperature of the air at the nozzle exit was measured using thermocouples. However, measuring the temperature of the work material during machining was challenging due to the movement of the heat source or work piece. Therefore, the temperature of the air near the tip of the nozzle was considered as the air temperature or jet temperature. This machining process involved a large number of variables, all of which directly and indirectly affected the machining results. For the purpose of this investigation, only the major variables that were easy to control were considered.

Table 4.8: Process Parameters

Parameters	Condition
Jet pressure (p)	4, 5 & 6 kgf/cm^2
Abrasive material (a)	Sic
Abrasive grain size (d)	40 µm
Nozzle diameter (D)	4 mm
Thickness of work piece (t)	5mm
Stand of distance (s)	5, 6, & 7 mm
Air temperature (T)	30℃ - 50℃

Soda lime glass Sic (abrasive particles)

Fig 4.12: Soda-lime glass (work material) and SiC (abrasive particles)

For the purpose of the present investigation, only major and easy to control variables like air temperature, stand-off distance and pressure were considered. The other experimental parameters were kept constant throughout the machining process as shown in Table 6.1.

4.13 AHAJM PROCESS:

In the process of abrasive hot air jets machining, abrasive particles are directed towards the work material at a high velocity. These particles are carried by a carrier gas or air. The high velocity stream of abrasives is achieved by converting the pressure energy of the carrier gas or air into kinetic energy, resulting in a high-velocity jet. The abrasive jet is directed onto the work material in a controlled manner through nozzles. The high-velocity abrasive particles remove the material through a combination of micro-cutting action and brittle fracture of the work material. Abrasive hot air jets machining (AHAJM) involves the removal of material through the impact erosion caused by a concentrated high-velocity stream of grit abrasives entrained in a high-velocity gas stream. It differs from shot or sand blasting as it utilizes finer abrasive grits and allows for more effective control of parameters, resulting in better overall control. Please refer to the figure below for a visual representation of the machined work pieces.

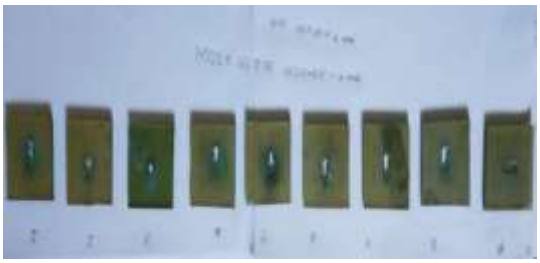

Fig 4.13: Machined work pieces

5 DATA COLLECTION AND CALCULATIONS

In the present work MRR (Q) is calculated on mass basis for which the formula used is

$Q = (W_B - W_A) / (MT)$

Where W_B is Weight of the workpiece before machining,

W_A is Weight of the workpiece after machining and,

MT is Machining time for the work material

Model Calculations for MRR:

For thickness of glass is 5 mm; nozzle dia. is 4mm; SOD is 5mm and pressure 4kgf/cm^2,

Q = (31.7-28.34)/27

Q =0.124 (g/s)

Model Calculations for Ra:

For thickness of glass is 5 mm; nozzle dia. is 4mm; SOD is 5mm and pressure 4kgf/cm^2,

$Ra = \left(\frac{0.329+0.356+0.276+0.357}{4}\right)$

Ra = 0.329 µm

6 RESULTS AND DISCUSSION

Experiments were conducted to study the effect of MRR and Surface roughness with respect to SOD, Pressure and temperature and the results were obtained for grooving using AHAJM. The effect of parameters like SOD, Pressure and temperature on MRR and Surface roughness (Ra) of the material using abrasive hot air jet machining was similar to that of AHAJM as discussed earlier in literature. Thickness of work material (t) is not a significant parameter influencing MRR and the surface roughness so thickness of work material is fixed as 5mm.In this work, the effect of air temperature on MRR and surface roughness for glass material at different operating conditions for grooving isfocused. The effecting parameters and responses considered in experimental investigation are

SOD - Standoff distance (mm)
HAT - Hot air temperature (°C)
P - Nozzle pressure (kgf/cm^2)
W_b - Weight of the work piece before machining (g)
W_a - Weight of the work piece after machining (g)
R_a - Surface roughness (µm)
MRR - Material removal rate (g/s),

The corresponding results obtained from experimental investigation were drafted as shown in below table 6.1: WORKPIECE SIZE 50*50*5.

Table 6.1: Consolidated values of experiment:

SOD	HAT	P	W_B	W_A	MT	MRR	Ra
5	30	4	31.7	28.34	27	0.124	0.329
5	40	5	32	28.3	28	0.132	0.359
5	50	6	31.9	28.67	26	0.159	0.343
6	30	4	29.4	28.33	32	0.134	0.487
6	40	5	29	28	30	0.196	0.452
6	50	6	29.2	28.62	26	0.303	0.441
7	30	4	29	28.4	33	0.018	0.413

7	40	5	29	28.05	31	0.029	0.384
7	50	6	29.4	28.07	26	0.031	0.328

Influence of air temperature on material removal rate. The air temperature was varied from 30^0C to 50^0C and the values of the other parameters were kept constant (when thickness of glass is 5 mm; nozzle dia. is 4mm; SOD is 5, 6, and 7mm and pressure 4, 5, and 6kgf/cm2) for the grooving process. Silicon carbide (Sic) of sizes 40 micron-m respectively, was used as abrasives formachining ofglass. Effects are varying HAT on MRR (when thickness of glass is 5 mm; nozzle dia. Is 4mm; SOD is 5mm and pressure 4kgf/cm^2) are tabulated in table6.2.

Table 6.2: HAT Vs MRR at SOD is 5mm and pressure 4kgf/cm^2

HAT (^{0} C)	MRR (g/s)
30	0.124
40	0.132
50	0.159

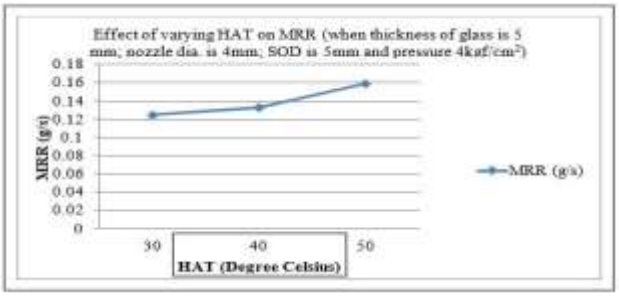

Fig 6.1: HAT Vs MRR at SOD is 5mm and pressure 4kgf/cm^2

Fig 6.1 shows the scattered plot of air temperature versus MRR. The MRR increases with the increase of the air temperature as shown in above figure. The trend observed in the curve indicates that the effect of air temperature on MRR is more significant above 50^0C and less significant at low temperature (30^0C). It can be found that the MRR at higher temperature (50^0C) is 0.8 times more than that of at lowtemperature. Effects of varying HAT on MRR (when thickness of glass is 5 mm, nozzle Dia is 4mm; SOD is 6mm and pressure 5kgf/cm^2) are tabulated in table6.3.

Table 6.3: HAT Vs MRR at SOD is 6mm and pressure 5kgf/cm^2:

HAT (^{0} C)	MRR (g/s)
30	0.134
40	0.196
50	0.303

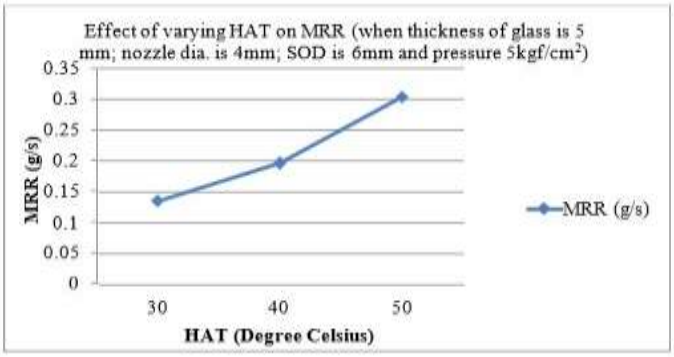

Fig 6.2: HAT Vs MRR at SOD is 6mm and pressure 5kgf/cm^2

Fig 6.2 shows the scattered plot of air temperature versus MRR. The MRR increases with the increase of the air temperature as shown in above figure. The trend observed in the curve indicates that the effect of air temperature on MRR is more significant above 50^{0}C and less significant at low temperature (30^{0}C). It can be found that the MRR at higher temperature (50^{0}C) is 0.5 times more than that of at lowtemperature. Effects of varying HAT on MRR (when thickness of glass is 5 mm, nozzle dia is 4mm; SOD is 7mm and pressure 6kgf/cm^2) are tabulated in table6.4.

Table 6.4: HAT Vs MRR at SOD is 7mm and pressure 6kgf/cm^2:

HAT (^{0} C)	MRR (g/s)
30	0.018
40	0.029
50	0.031

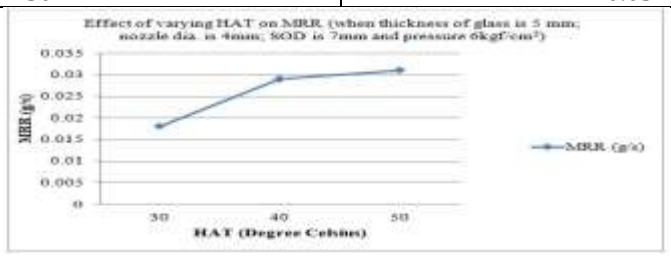

Fig 6.3: HAT Vs MRR at SOD is 7mm and pressure 6kgf/cm2

Fig 6.3 shows the scattered plot of air temperature versus MRR. The MRR increases with the increase of the air temperature as shown in above figure. The trend observed in the curve indicates that the effect of air temperature on MRR is more significant above 50^{0}C and less significant at low temperature (30^{0}C). It can be found that the MRR at higher temperature (50^{0}C) is 0.6 times more than that of at low temperature. Influence of Air Temperature on surface roughness. The air temperature was varied from 30^{0}C to 50^{0}C and the values of the other parameters were kept constant (when thickness of glass is 5 mm; nozzle dia. is 4mm; SOD is 5, 6, 7mm and pressure 4, 5, 6kgf/cm2) for the grooving process. Silicon carbide (Sic) of sizes 40 micron-m respectively, was used as abrasives for machining of glass. Effect of varying HAT on Ra (when thickness of glass is 5 mm; nozzle dia. is 4mm; SOD is 5mm and pressure 4kgf/cm2) are tabulated in table 6.5.

Table 6.5: HAT Vs Ra at SOD is 5mm and pressure 4kgf/cm^2

HAT (^{0} C)	Ra (µm)
30	0.329
40	0.359
50	0.343

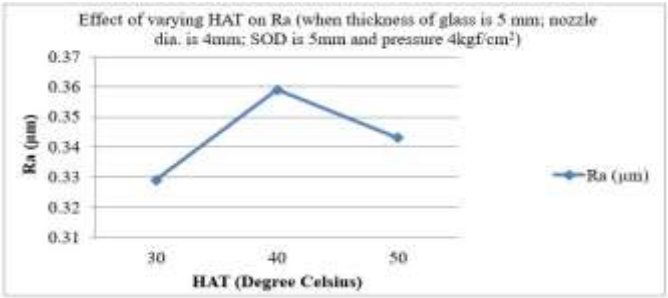

Fig 6.4: HAT Vs Ra at SOD is 5mm and pressure 4kgf/cm2

Fig 6.4 shows the scattered plot of air temperature versus Ra. The Ra increases with the increase of the air temperature as shown in above figure up to 40^{0}C then decreases with the increase of the air temperature. The trend

observed in the curve indicates that the effect of air temperature on Ra is more significant above 40^0C and less significant from 30^0C to 40^0C temperature. Effect of varying HAT on Ra (when thickness of glass is 5 mm; nozzle dia. is 4mm; SOD is 6mm and pressure 5kgf/cm^2) are tabulated in table6.6.

Table 6.6: HAT Vs Ra at SOD is 6mm and pressure 5kgf/cm^2

HAT (^{0} C)	Ra (µm)
30	0.487
40	0.452
50	0.441

Fig 6.5 shows the scattered plot of air temperature versus Ra. The Ra decreases with the increase of the air temperature as shown in above figure. The trend observed in the curve indicates that the effect of air temperature on Ra is more significant above 50^0C and less significant at low temperature (30^0C). It can be found that the Ra at higher temperature (50^0C) decreases by 1.2 times than that of at low temperature. Effect of varying HAT on Ra (when thickness of glass is 5 mm; nozzle dia. is 4mm; SOD is 7mm and pressure 6kgf/cm2) are tabulated in table 6.7.

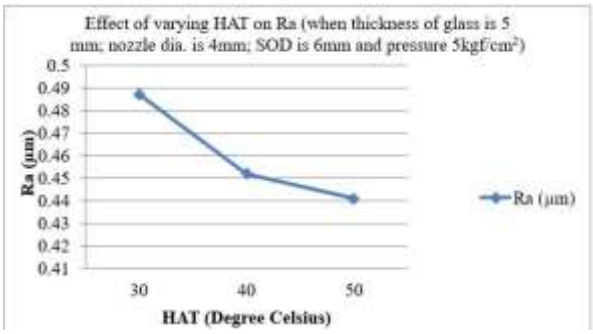

Fig 6.5: HAT Vs Ra at SOD is 6mm and pressure 5kgf/cm2

Table 6.7:HAT Vs Ra at SOD is 7mm and pressure 6kgf/cm2

HAT (^{0} C)	Ra (µm)
30	0.413
40	0.384
50	0.328

Fig 6.6: HAT Vs Ra at SOD is 7mm and pressure 6kgf/cm2

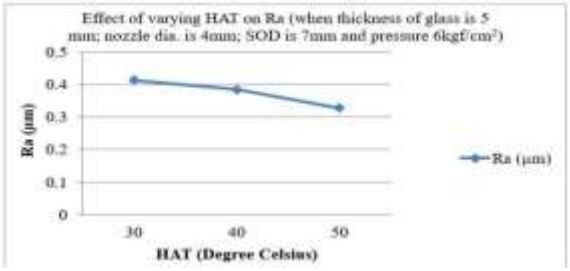

Fig 6.6 shows the scattered plot of air temperature versus Ra. The Ra slightly decreases with the increase of the air temperature as shown in above figure. The trend observed in the curve indicates that the effect of air temperature on Ra is more significant above 50^0C and less significant at low temperature (30^0C). It can be found that the Ra at higher temperature.

7 Conclusions

This project work aims to investigate the impact of air temperature on the material removal rate (MRR) and quality of the machined surface. The conclusions drawn from the experimental investigation are as follows. The influence of air temperature on MRR is more pronounced at temperatures above 500C, while it becomes less significant at lower temperatures. The MRR increases as the air temperature rises. When hot air is directed towards the target, it raises the temperature of the target, leading to an increase in the size of radial cracks caused by the impact of abrasive material. This, in turn, facilitates the removal of a larger amount of chips from the work material. Consistent with this observation, the present study demonstrates that the MRR of the material is higher at high temperatures compared to low temperatures. At low temperatures, crack initiation occurs due to the brittle nature of the material. However, as the temperature increases, it has been observed that deep chipping followed by plastic deformation takes place. Consequently, the erosion rate increases, highlighting the influence of hot air in enhancing the MRR.

It was observed that increasing the temperature of the air resulted in a decrease in the roughness of the machined surface. Additionally, it was noted that the surface roughness (Ra) value is particularly low at 500C. The impact of hot air with abrasives raises the temperature of the target, leading to increased plastic deformation on the target surface. This, in turn, facilitates the removal of larger chips from the material. The removal of material in the form of larger cracks creates a new, smoother bottom surface on the target, thereby reducing the roughness of the machined surface. The plasticity of the subsurface at the target is also increased due to the rise in erodent temperature, resulting in a smoother surface.

It is evident that air temperature not only affects the MRR but also has an impact on the roughness of the machined surface.

Future Scope

The above experimental investigation on AHAJM can be extended for higher temperatures with different abrasive materials and different abrasive grain sizes in order to explore the other process variables.

References

1. Achtsnick, M.Geelhoed, P.F. (2005) Modeling and evaluation of the micro abrasive blasting process. Wear, 259:84-269.
2. Balasubramaniam, R. Krishnan, J. Ramakrishnan, N. (1999) An experimental study on the abrasive jet deburring of cross-drilled holes. Journal of Material Processing Technology, 91: 178–182.
3. El-Domiaty, A. Abid El-Hafez, H.M. Shaker, M.A. (2009) Drilling of glass sheets by abrasive jet machining. World Academy of Science Engineering and Technology, 56:61– 67.
4. Ramachandran, N. Ramakrishnan, (1993) Abrasive jet machining upcoming technology in metal processing a review. Journal of Material Processing Technology, 39(1–2): 21–30.
5. Zhang, L. Kuriyagawa, T. Yasutomi, Y. Zhao, (2005) Investigation into micro abrasive intermittent jet machining. International Journal of Machine Tools &Manufacture, 45: 873–879
6. Z Park, D.S. Cho, M.W. Lee, H. Cho, W.S. (2004) Micro-grooving of glass using micro–Abrasive Jet Machining. Journal of Material Processing Technology, 146(2): 234–240.
7. Getu, H. Ghobeity, A. Spelt, J.K. Papini, M. (2011) Thermal analysis of cryogenically assisted abrasive jet micromachining of PDMS. International Journal of Machine Tools & Manufacture 1: 721–730.
8. Ghobeity, A. Papini, M. Spelt, J.K. (2007) Computer simulation of particle interference in abrasive jet micro machining. Wear, 263: 265–269.
9. Ghobeity, A. Krajac, T. Burzynski, T. Papini, M. Spelt, J.K. (2008) Surface evolution models in abrasive jet micro-machining. Wear, 264: 185–198.
10. Ghobeity, A. Spelt, J.K. Papini J. (2008) Abrasive jet micromachining of acrylic and polycarbonate polymers at oblique angles of attack. Wear, 265: 888–901.
11. Fan, J.M. Wang, C.Y. Wang, J. (2009) Modeling the erosion rate in micro abrasive air jet Machining of glasses. Wear, 266: 968–974.
12. Fan, J.M. Li, H.Z. Wang, J. Wang, C.Y. (2011) A study of the flow characteristics in micro abrasive jets. Experimental Thermal and Fluid Science, 35: 1097–1106.
13. Shafiei, N Getu H, Sadeghian, A. Papini, M. (2009) Computer simulation of developing abrasive jet machined profiles including particle interference. Journal of Material Processing Technology, 209: 4366–4378.

14. Evans, A. Gulden, M. Rosenblatt, M. (1978) Impact damage in brittle materials in the elastic– plastic response regime. Proceedings of the Royal Society of London, 361: 343–365.
15. Marshall, D.B. Lawn, B.R. Evans, G. (1982) Elastic=Plastic indentation damage in ceramics: The lateral crack system. Journal of American Ceramic Society, 65(11): 561– 566.
16. Zhou, J.R. Bahadur, S. (1995) Erosion characteristics of alumina ceramics at high temperatures. Wear, 181–183: 178–188.
17. Wensink, H.Elwenspoek, M.C. (2002) a closer look at the ductile-brittle transition in solid particle erosion. Wear, 253: 1035–1043.
18. Slikkerveer, P.J Bouten, C.P. Veld, F.H. Scholten, H. (1998) Erosion and damage by sharp particles. Wear, 217: 237–250.
19. Slikkerveer, P.J. (2002) Mathematical modeling of erosion by powder blasting. Surveys on Mathematics for Industries, 10: 89–105.
20. Zhou, J.R. Bahadur, S. (1995) Erosion characteristics of alumina ceramics at high temperatures. Wear, 181–183: 178–188.
21. Muralidhar, S.Pal, S. Mittal, R.K. Kale, S.R. (1982) A Study of thermal cutting of glass. Journal of American Ceramic Society, 8: 2166–2176.
22. Shahani, A.R. Seyyedian, M. (2004) Simulation` of glass cutting with an impinging hot air jet. International Journal of Solids and Structures, 41: 1313–1329.
23. Prakash, E.S. Sadashivappa, K. Singaperumal, M. (2001) Non conventional cutting of plate glass using hot air jet: Experimental studies. Mechatronic, 11: 595–615.Another reference